Metagenomics and metabolic modelling of anaerobic digestion coupled microbial electrolysis cell with different electrode types and voltage levels

D. Sanguineti[1], S. Campanaro[1], D. Hidalgo[2], M. A. Sanchez[2], G. Zampieri[1], R.A. Timmers[2], L. Treu[1]

[1]Department of Biology, University of Padova, Padova, 35129, Italy
[2]Circular Economy Area, CARTIF Technology Centre, 47151 Valladolid, Spain
Keywords: Anaerobic digestion, Microbial-electrolysis cell, Metagenomics, Metabolic modelling
Presenting author email: davide.sanguineti@studenti.unipd.it

Introduction

Coupling Anaerobic Digestion (AD) with Microbial Electrolysis Cell (MEC) is a promising approach to enhance process performance and increase the CH_4 fraction in biogas. A MEC is composed of an anode and a cathode, occasionally separated by a semi-permeable membrane (Swaminathan et al., 2024), with microbes growing both in the liquid phase and attached to the electrode surface. Integrating AD with MEC (AD-MEC) has been shown to improve CH_4 productivity, process stability, and biogas purity by accelerating the rate of CO_2 conversion to biomethane (Zakaria and Dhar, 2019).

Electroactive bacteria (EAB) are a key factor in enhancing the performance of AD-MEC systems. These organisms are capable of extracellular electron transfer, that is, shuttling electrons from intracellular compounds to extracellular acceptors, or conversely, from extracellular donors to intracellular compounds (Logan et al., 2019). While *Geobacter* spp. are the most extensively studied EAB, diverse taxa such as *Trichococcus* spp. and *Exiguobacterium* spp. have also been observed in AD-MEC systems (Joshi et al., 2024; Liu et al., 2025; Xiao et al., 2024). There are three main mechanisms which EAB can improve CH_4 production: i) direct interspecies electron transfer (IET) with electrotrophic methanogens, ii) electrode-mediated IET, and iii) H_2-mediated IET (Zakaria and Dhar, 2019). However, it remains unclear which pathway is most effective for CH_4 production, or how the predominance of a given mechanism relates to community composition and metabolic interactions. Unraveling these metabolic and interaction networks is therefore crucial to identify and enrich microbial traits associated with performance enhancement in AD-MEC systems.

In this work, microbial samples were collected from seven lab-scale reactors initialized with the same inoculum. In each reactor a specific combination of applied voltage (0.0V, 0.5V or 0.7V) and electrode type (graphite plate or graphite felt) was tested. Genome-centric metagenomics was applied to reconstruct the community composition in each samples, identifying dominant species in these systems. The functional composition of the community was characterized, and genome scale metabolic models were reconstructed for each species. Community-level metabolic simulations were performed to identify metabolic exchanges driving species coexistence and process efficiency. Finally, *in silico* enrichment with EAB was identified as a promising strategy to improve CH_4 production.

Materials and Methods

Six reactors were operated as anaerobic digestors with electrodes with a specific combination of applied voltage (0.0V, 0.5V or 0.7V) and electrode type (graphite plate or graphite felt). One reactor was operated as a reference without electrode. Reactors were operated in a semi-continuous (fed-batch) fashion. The system was fed with glucose as the carbon source. Each day, 45 mL of the reactor content was removed and replaced with an equal volume of glucose solution (20 g/L). In the second phase the OLR was doubled to 2 g glucose/L/day, and the HRT was reduced to 10 days. To support microbial growth and maintain stable reactor conditions, nutrients and phosphate buffer were added once a week. Reactor were operated for 100 days and microbial samples were collected at the end of the experiment.

Metagenome-assembled genomes (MAGs) were reconstructed using a previously established pipeline (Centurion et al., 2024). Briefly, first sequencing reads are quality-filtered and co-assembled into contigs. Contigs are binned into potential microbial genomes using multiple binning tools. Bins are clustered into species' level genomes according to sequence identity, and the best species representative MAG is selected based on quality criteria. Species-level community representation is obtained by mapping sequencing reads to the set of MAGs and using mapped read counts as proxies for relative abundances.

For each MAG, draft genome-scale metabolic models (GEMs) were built using Gapseq v1.2 (Zimmermann et al., 2021) and refined by applying the gap-filling function. Species were filtered to include only those with a Relative Abundance (RA) equal or higher than 1 % in at least one condition. For each GRT condition, community-level metabolic models were generated with Micom v0.33.1 (Diener et al., 2020) by merging GEMs of the selected abundant species. Uptake reaction constraints were imposed to match CO_2 and Glucose import rates with experimental data. *In-silico* medium was predicted using an *Ad-hoc* optimization strategy and models were solved using a modified version of the cooperative trade-off strategy, as previously described (Sanguineti et al., 2025).

To model electron transfer mechanisms, Species encoding pilA sequences that conformed to the criteria defined in literature were classified as putative EAB (Bray et al., 2020), and they were assigned an acetate oxidation reaction resulting in the production of ATP, CO_2, H+. Methanogens capable of electromethanogenesis were defined based on the literature (Zakaria and Dhar, 2019), and they were assigned a reaction to generate CH4 from protons, electrons and CO_2.

Simulation of species bioaugmentation was performed collecting reference genomes of known EAB. Their GEM was built with Gapseq and introduced in the MICOM community model with a specified abundance level, and the aforementioned acetate oxidation reaction was included. All other model parameters and constraints were kept fixed, and CH_4 community export was evaluated as a measure of process efficiency.

Results and discussion

Microbial composition was reconstructed into 306 species-level high quality MAGs, with approximately half of them deriving from batch samples. Average completeness and contamination are, respectively, 82% (±15%) and 2% (±2%). Average alignment rates are 67% (±4%) indicating a good recovery of the microbial community. Fermentative bacteria *Brooklawnia* sp. and *Bifidobacterium subtile* clearly dominate the community, with average RA of 24% (±14%) and 19% (±14%), respectively (Figure 1A). Focusing on the methanogens found in this system, *Methanothrix sohegenii* (known acetoclastic), *Methanobacterium congolense, Methanobacterium formicicum and Methanobacteriaceae sp.* (known hydrogenotrophic methanogens) are the most relevant, while displaying RA levels lower than 5%. Notably, in the condition where voltage is applied, the hydrogenotrophic *Methanobacterium spp*. are enriched, since they thrive in a hydrogen-richer environment (Figure 1B**)**. Six putative EAB were identified, with *Nanosynbacter* spp. being the most abundant and enriched in felt-type electrodes when voltage is applied, although the RA was never higher than 5%. The community composition differs notably across experimental conditions, as shown in the multidimensional scaling of species abundances (Figure 1C). Separation was observed according to electrode type (felt vs plate) and applied voltage (blank and Felt0V vs others), indicating that both parameters significantly influence the establishment and stability of microbiome states.

Community-level GSMMs were built using reconstructed species with RA $\geq$ 1% in at least one condition, resulting in a set of 37 species within the MEC systems. Depending on the sample, these models comprised between 30376 and 48379 biochemical reactions distributed across 22 to 33 species. As shown in (Figure 2A), CH_4 production predicted by the models aligned with the observed values. Moreover, species-specific replication rates across conditions inferred based on the sequencing data (Joseph et al., 2022) positively correlate with model-predicted growth rates (Figure 2B). Overall, reconstructed models reasonably reflect experimental data. Figure 3A shows, for conditions with an applied voltage of 0.5 V, producers and consumers of compounds of interest, such as H_2, CH_4, and acetate, as well as electrons. Patterns in exchange fluxes clearly differentiate between the two types of electrode (felt and plate), independently from the voltage applied. In particular, the main CH4 producer in felt sample is s__Methanothrix_soehngenii_1 via acetoclastic methanogenesis, while in plate sample multiple methanogens participate in CH_4 generation. This observation reflects the differences in RA evenness observed in the two conditions; in plate samples methanogens' RA is more evenly distributed across species (Figure 1B). Notably, felt samples have, in general, higher levels of CH_4 production (Figure 2A), suggesting that competition between methanogens might be deleterious for process performance. Concerning electrochemical mechanisms, electrons generated by *Nanosynbacter* spp. mainly participate in H_2 generation at the cathode, although *M. soehngenii* spp. perform electromethanogenesis across samples. In general, both concerning H_2 generation and CH_4 production, electrochemical mechanisms have an extremely marginal effect on CH_4 production.

In order to assess whether enrichment with EAB might result in higher bioreactor performance, we performed in-silico bioaugmentation simulations of several known EAB: *Geobacter sulfurreducens, Geobacter metallireducens, Calditerrivibrio nitroreducens, Desulfurivibrio alkaliphilus and Syntrophus aciditrophicus* (Bray et al., 2020). Results of the bioaugmentation simulations are shown in Figure 3B. In conditions where voltage is applied, most EAB have a positive impact on CH_4 production, which positively correlates with their abundance (Spearman $R = 0.56$, p-value < 0.01). Notably, plate samples have, on average, lower CH_4 production than felt samples, as observed in real data (Figure 2A). The highest performances are achieved in FB_Felt07V, with maximum production obtained with bioaugmentation of G. sulfurreducens at RA 90%, with CH_4 export of 2.45 mmol/h, more than ten times higher than the experimentally-observed maximum production. Simulation results thus suggest that bioaugmenting the community with EAB would allow a more efficient exploitation of the MEC system in the AD reactor, thus resulting in higher performances.

Conclusions

An AD-MEC microbial community was analyzed and modelled throughout different experimental conditions, and potential solutions to improve process performance were *in-silico* explored. Notably, known EAB were not identified in the microbial community, and putative EAB have low relative abundance. This may be due to the

glucose feeding, as it tends to enrich fermentative bacteria such as *Brooklawnia* sp. and *Bifidobacterium subtile* (Zakaria and Dhar, 2019). In accordance with abundance data, simulations of bioaugmentation with culturable EAB, such as *Geobacter sulfurreducens*, suggest that enriching the community with these species can allow a more efficient exploitation of the MEC properties, and could improve CH4 production up to ten times the observed values. results from community-level FBA indicate that electrochemical mechanisms concur only marginally to CH_4 production.

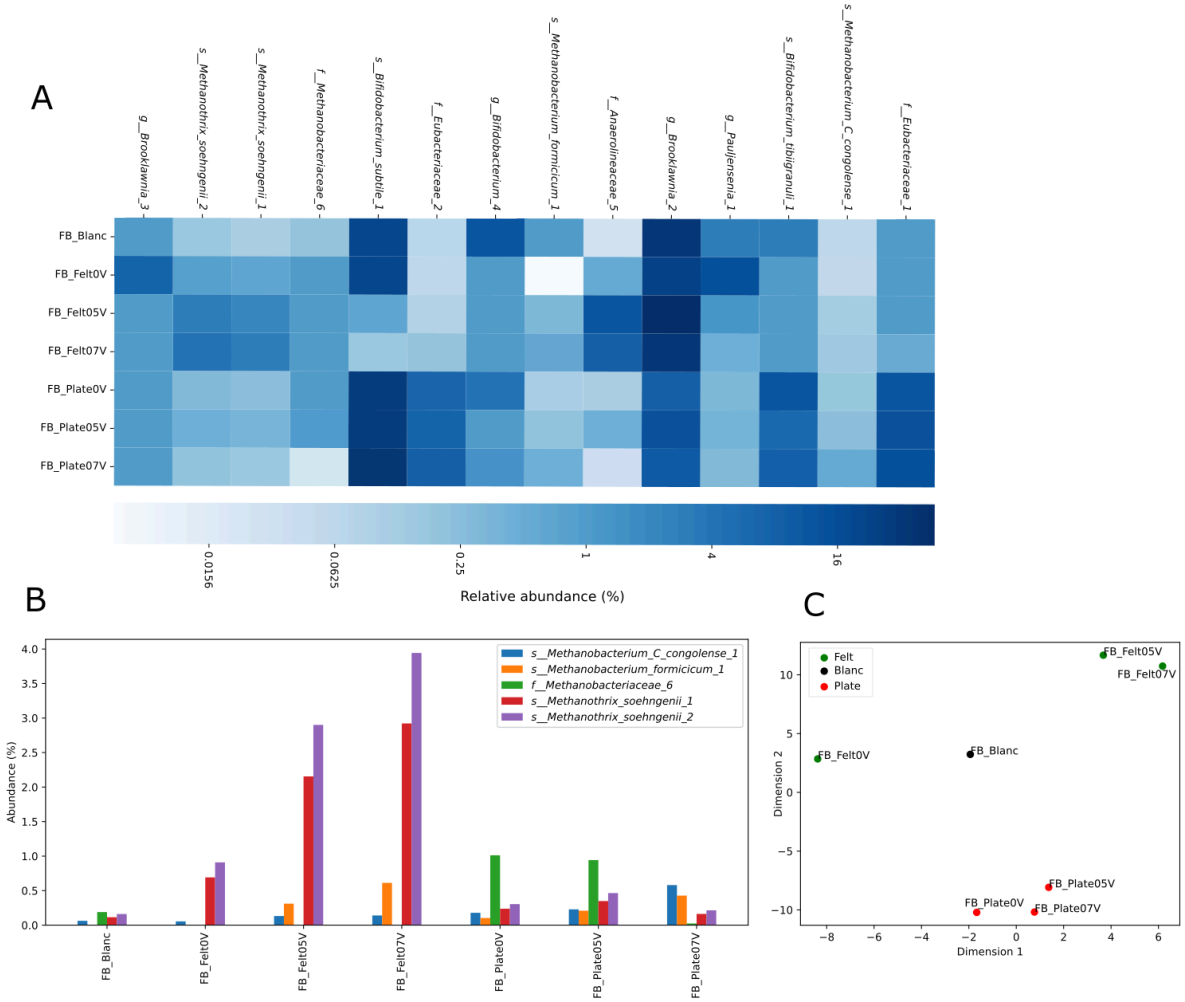

Figure 1. A) Heatmap displaying RAs across GRT conditions (x-axis) for species with RA higher than 7.5% in at least one sample (y-axis) and the 5 most abundant methanogens. B) RA (y-axis) of the dominant methanogenic species across conditions, as indicated on the x-axis. C) Multidimensional scaling applied to microbial RA. Samples are marked with different colors, as indicated in the figure legend.

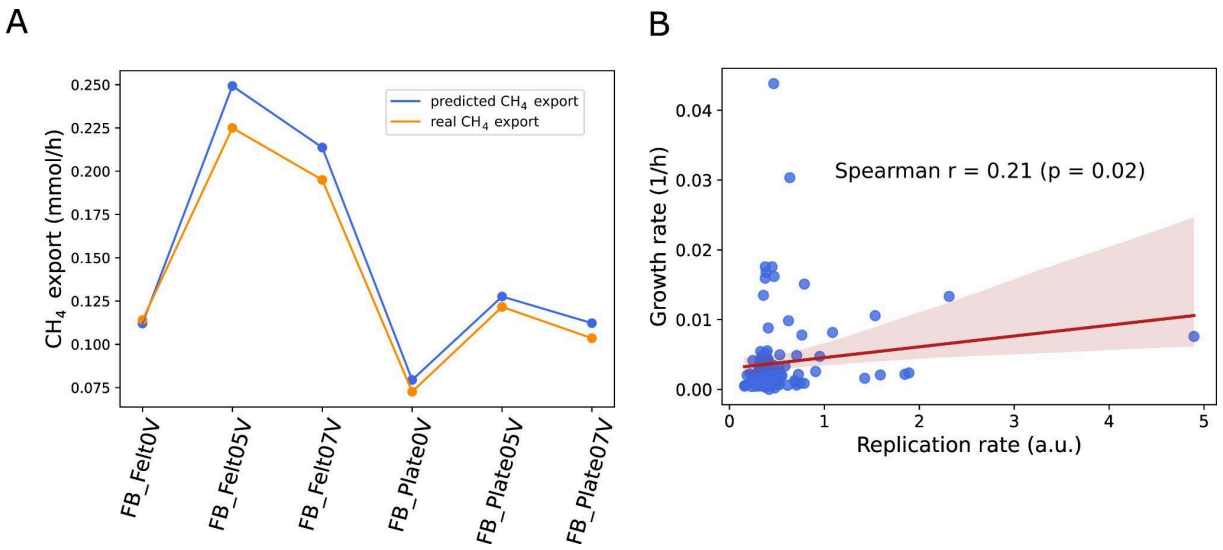

Figure 2. A) The y-axis displays the observed CH_4 production rate and the model-predicted CH_4 export one (y-axis) across conditions (x-axis). B) Scatterplot (blue dots) and fitted linear regression model (red line) between coverage-inferred replication rates (x-axis) and model-predicted growth rates (y-axis). On top of the plot, Spearman correlation coefficient and associated p-value are displayed.

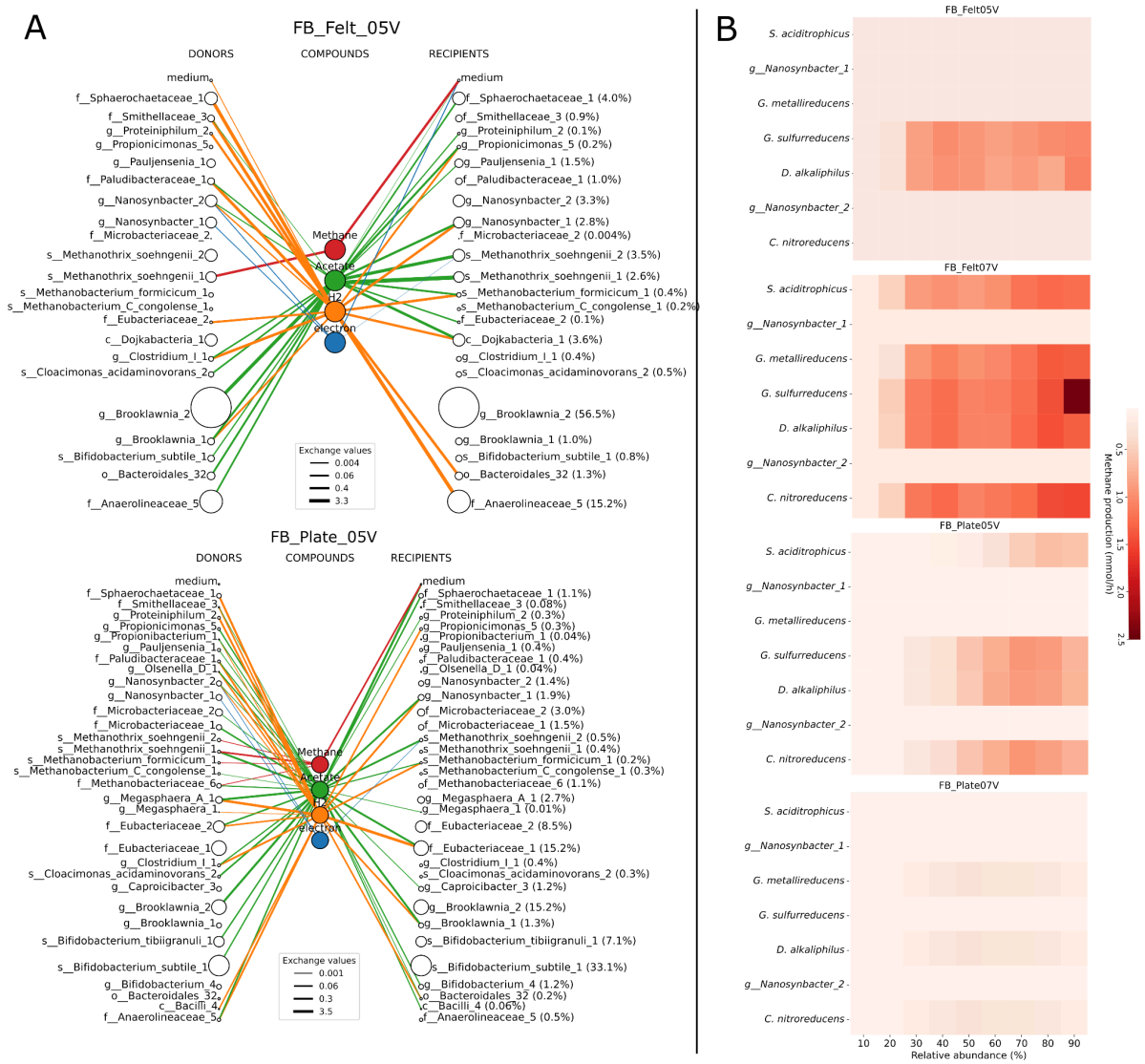

Figure 3. A) Metabolic exchanges of compounds of interest (center). Circle size indicates the RA of the species under examination, while line width is proportional to flux value, as indicated in the figure legend. Lines starting from DONORS (left) represent production of the corresponding compound, while lines from RECIPIENTS (right) represent consumption. Medium's production of H2 corresponds only to cathodic reduction of protons. B) Predicted CH_4 production in each sample upon bioaugmentation with the indicated species and RAs. Values below baseline production are rounded up to the original levels.

References

Bray, M.S., Wu, J., Padilla, C.C., Stewart, F.J., Fowle, D.A., Henny, C., Simister, R.L., Thompson, K.J., Crowe, S.A., Glass, J.B., 2020. Phylogenetic and structural diversity of aromatically dense pili from environmental metagenomes. Environ. Microbiol. Rep. 12, 49–57. https://doi.org/10.1111/1758-2229.12809

Centurion, V.B., Rossi, A., Orellana, E., Ghiotto, G., Kakuk, B., Morlino, M.S., Basile, A., Zampieri, G., Treu, L., Campanaro, S., 2024. A unified compendium of prokaryotic and viral genomes from over 300 anaerobic digestion microbiomes. Environ. Microbiome 19. https://doi.org/10.1186/s40793-023-00545-2

Diener, C., Gibbons, S.M., Resendis-Antonio, O., 2020. MICOM: Metagenome-Scale Modeling To Infer Metabolic Interactions in the Gut Microbiota. mSystems 5, 10.1128/msystems.00606-19. https://doi.org/10.1128/msystems.00606-19

Joseph, T.A., Chlenski, P., Litman, A., Korem, T., Pe'er, I., 2022. Accurate and robust inference of microbial growth dynamics from metagenomic sequencing reveals personalized growth rates. Genome Res. 32, 558–568. https://doi.org/10.1101/gr.275533.121

Joshi, J., Bhatt, P., Kandel, P., Khadka, M., Kathariya, S., Thapa, S., Jha, S., Phaiju, S., Bajracharya, S., Yadav, A.P., 2024. Integrating microbial electrochemical cell in anaerobic digestion of vegetable wastes to enhance biogas production. Bioresour. Technol. Rep. 27, 101940. https://doi.org/10.1016/j.biteb.2024.101940

Liu, C., Cao, Q., Luo, X., Yan, S., Sun, Q., Zheng, Y., Zhen, G., 2025. In-depth exploration of microbial electrolysis cell coupled with anaerobic digestion (MEC-AD) for methanogenesis in treating protein wastewater at high organic loading rates. Energy Convers. Manag. 323, 119152. https://doi.org/10.1016/j.enconman.2024.119152

Logan, B.E., Rossi, R., Ragab, A., Saikaly, P.E., 2019. Electroactive microorganisms in bioelectrochemical systems. Nat. Rev. Microbiol. 17, 307–319. https://doi.org/10.1038/s41579-019-0173-x

Sanguineti, D., Chatzis, A., Zampieri, G., Gaspari, M., Kougias, P.G., Campanaro, S., Treu, L., 2025. Modelling microbial and metabolic shifts in trickle bed reactor biomethanation at decreasing gas retention times. Chem. Eng. J. 522, 167574. https://doi.org/10.1016/j.cej.2025.167574

Swaminathan, P., Ghosh, A., Sunantha, G., Sivagami, K., Mohanakrishna, G., Aishwarya, S., Shah, S., Sethumadhavan, A., Ranjan, P., Prajapat, R., 2024. A comprehensive review of microbial electrolysis cells: Integrated for wastewater treatment and hydrogen generation. Process Saf. Environ. Prot. 190, 458–474. https://doi.org/10.1016/j.psep.2024.08.032

Xiao, B., Wang, X., He, E., Zuo, Y., Wan, L., Li, L., 2024. Effects of microbial electrolysis cell on anaerobic digestion of food waste: Acidification and recovery. Fuel 369, 131756. https://doi.org/10.1016/j.fuel.2024.131756

Zakaria, B.S., Dhar, B.R., 2019. Progress towards catalyzing electro-methanogenesis in anaerobic digestion process: Fundamentals, process optimization, design and scale-up considerations. Bioresour. Technol. 289, 121738. https://doi.org/10.1016/j.biortech.2019.121738

Zimmermann, J., Kaleta, C., Waschina, S., 2021. gapseq: informed prediction of bacterial metabolic pathways and reconstruction of accurate metabolic models. Genome Biol. 22, 81. https://doi.org/10.1186/s13059-021-02295-1

De Bernardini, N., Zampieri, G., Campanaro, S., Zimmermann, J., Waschina, S., Treu, L., 2024. pan-Draft: automated reconstruction of species-representative metabolic models from multiple genomes. Genome Biol. 25. https://doi.org/10.1186/s13059-024-03425-1